GEOPHYSICAL RESEARCH LETTERS, VOL. 22, NO. 4, PAGES 349-352, FEBRUARY 15, 1995

The structure of the distant geomagnetic tail during long periods of northward IMF

J. Raeder, R. J. Walker, and M. Ashour-Abdalla[1]

Institute of Geophysics and Planetary Physics, University of California, Los Angeles

Abstract. We have used a newly developed, parallelized, global MHD magnetosphere - ionosphere simulation model with a 400 R_E long tail to study the evolution, structure, and dynamics of the distant magnetotail during extended periods of northward IMF. We find that the tail evolves to a nearly time stationary structure about one solar wind transit time after the IMF turns northward. Four regions of different magnetic topology can be distinguished which extend at least to the end of the simulation box at 400 R_E. Besides lobe field lines and open solar wind field lines tailward of an X-line, there is a broad boundary layer of closed field lines which we call the tail flank boundary layer (TFBL). Just inside the TFBL there is a region of closed field loops. Besides the X-line we find two O-lines which are enclosed by the closed field loops and are roughly aligned with the tail axis. Together they form a U shaped separator between the northward and the southward plasma sheet fields.

Introduction

The geomagnetic tail is one of the most dynamic regions of the Earth's magnetosphere and is probably the least understood. This is particularly true for the distant tail, i.e., the part of the tail that extends beyond the lunar orbit. The distant tail has been visited by only a few spacecraft, and ISEE 3 and GEOTAIL are the only probes to spend an extended amount of time there. Besides the scarcity of data from the distant tail there exists a problem in analyzing those observations because the tail is very unsteady and internal magnetospheric boundaries in the distant tail involve very subtle changes in plasma and field parameters. It is difficult to determine the position of a spacecraft with respect to the internal plasma boundaries because of the motion of the tail in response to changes in the solar wind dynamic pressure and direction, as well as the possible intrinsic instability of the tail. Also, determining the magnetic topology (i.e., open versus closed field lines) becomes increasingly more difficult at greater distances from the Earth. In spite of these difficulties, ISEE 3 provided a great deal of information which allowed us for the first time to determine the average plasma and field parameters of the distant tail [see review by Tsurutani et al., 1986]. Although the ISEE 3 data confirmed the concept of an open magnetosphere and the extension of the near-Earth tail features into the distant tail, one unexpected finding of the mission was the frequent occurrence of tailward plasma sheet flows associated with positive B_z [Slavin et al., 1985, 1987; Siscoe et al., 1987; Heikkila, 1987] in contrast to the predictions for an open magnetosphere [Dungey, 1961]. Slavin found that, by ordering the average B_z values into GSM-X bins, the average B_z values decrease more or less monotonically as a function of tail distance and become negative beyond -210 R_E.

[1]Also at Physics Dept., University of California, Los Angeles

Paper number 94GL03380
0094-8534/95/94GL-03380$03.00

By taking into account the Y dependence, he found that the average B_z value becomes negative at smaller distances from the Earth near the tail axis and remains positive up to -225 R_E closer to the flanks. Based on these findings he proposed a tail model in which a U-shaped X-line exists in the plasma sheet, has its apex near -120 R_E and converges towards the tail flanks at larger distances.

Because of the large variations in the plasma and field parameters the observed statistical averages cannot be assumed to represent a steady state of the tail. The large variations indicate that a steady state tail may be a rare and exceptional case. During magnetically quiet times, however, the tail dynamics generally cease and a well ordered structure is more likely to develop. We have therefore assumed a steady northward IMF for this study.

The Global MHD - Ionosphere Model

For this study we use a newly developed global MHD code which also includes an ionospheric model for the closure of field aligned currents. In order to accommodate the large simulation volume with a 400 R_E tail and long simulation times together with good resolution, the simulation code was parallelized for MIMD (Multiple Instruction - Multiple Data) machines by using a domain decomposition technique. We will only briefly outline the model here; a more detailed description will be published elsewhere. The model solves the ideal MHD equations for the magnetosphere and a potential equation for the ionosphere. However, because of numerical effects, diffusion and resistive effects occur in the MHD solutions; these permit viscous interactions and also magnetic field reconnection.

The magnetospheric (MHD) part of the model is solved by a finite difference method which is conservative for the gas-dynamic part of the MHD equations. The $j \times B$ and $E \cdot j$ terms are treated as source terms. Although full energy conservation cannot be guaranteed by this treatment, mass density, momentum, and plasma energy are conserved to round-off error. Test calculations for shock tube problems show that the total energy is conserved almost perfectly. The numerical grid is rectangular and nonuniform with the highest spatial resolution near the Earth (about 0.5 R_E). It extends 30 R_E in the sunward direction, 400 R_E in the tailward direction and 50 R_E in the Y and Z directions. The gas-dynamic part of the equations is spatially differenced by using a technique in which fourth order fluxes are hybridized with first order (Rusanov) fluxes [Harten and Zwas, 1972; Hirsch, 1990]. The magnetic induction equation is treated differently to ensure $\nabla \cdot B = 0$ by following a method outlined by Evans and Hawley [1988] that conserves $\nabla \cdot B$ exactly. The time stepping scheme for all variables consists of a low order predictor with a time centered corrector, which is second order accurate in time. The outer boundary conditions are fixed at the given solar wind values on the upstream side. At the other boundaries we apply open, i.e., zero normal derivative, boundary conditions.

The inner boundary, where the MHD quantities are connected to the ionosphere, is taken to be a shell of radius 3.7 R_E centered on the Earth. The choice of this radius is a compromise and guided by numerical necessities, such as extraneously high Alfvén speeds and very large magnetic field gradients closer to the Earth. However, it allows for the proper mapping of all relevant field aligned current systems. Inside this shell

we do not solve the MHD equations, but assume a static dipole field. The important physical processes within the shell are the flow of field aligned currents (FACs) and the closure of these currents in the ionosphere. At each time step we map the magnetospheric FACs from the 3.7 R_E shell onto the polar cap using a static dipole field. We then use the FACs as input for the ionospheric potential equation:

$$\nabla \cdot \underline{\underline{\Sigma}} \cdot \nabla \Phi = -j_{\parallel} \sin I$$

which is solved on the surface of a sphere with 1 R_E radius. Here Φ denotes the ionospheric potential, $\underline{\underline{\Sigma}}$ is the tensor of the ionospheric conductance, $j_{\parallel}$ is the mapped FAC with the downward current considered positive and corrected for flux tube convergence, and I is the inclination of the dipole field at the ionosphere. The boundary condition $\Phi = 0$ is applied at the equator. The ionospheric Hall and Pedersen conductances Σ_H and Σ_P which enter the conductance tensor $\underline{\underline{\Sigma}}$ [see e.g., Kamide and Matsushita, 1979] are given by a static analytic model that accounts for EUV and diffuse auroral contributions and is similar to the one used by Rasmussen and Schunk [1987]. Once the potential equation is solved the ionospheric potential is mapped to the 3.7 R_E shell and used as a boundary condition for the magnetospheric flow by taking $v = (-\nabla\Phi)\times B/B^2$. The initial conditions for the magnetic field are constructed from the superposition of the Earth's dipole over a mirror dipole, such that B_x vanishes at x = 16 R_E. Sunward of the tangential discontinuity at 16 R_E the field is replaced by the initial solar wind field. This procedure ensures a divergence-free transition from the constant solar wind field to the Earth's dipole field. The simulation box is initially filled with tenuous (0.1 cm^{-3}) and cold (5000^0 K) plasma of zero velocity, except for the near-Earth region, where the density varies as a function of geocentric distance, $\rho \sim R^{-3}$. The solar wind flow (v=400 km s^{-1}, ρ=6.75 amu cm^{-3}, T=50000^0 K, B_z=-5 nT) is switched on at the sunward boundary at time t=0, and the system is allowed to evolve under these southward IMF conditions for 2 hours, which is somewhat more than is required for the solar wind to pass once through the simulation box. By comparing runs with different initial conditions we found that the specific initial conditions have only a minimal effect on the structure of the magnetosphere after 2 hours of southward IMF. The southward IMF conditions let a neutral line (at about x = -25 R_E) and fast tailward flows to evolve, which clear the tail of any structures that are there as a result of the initial conditions. Then we switch the IMF to 5 nT northward and study the evolution of the tail.

Results

Figure 1 shows a perspective view of the magnetosphere after the first two hours of southward IMF. In the equatorial plane we have color coded the logarithm of the temperature and have also plotted flow vectors. The bow shock is clearly discernible, as is the hot plasma sheet. In the vertical cuts at x = -200 R_E and x = -360 R_E we have color coded the x component of the magnetic field. Areas with large B_x indicate the lobes and their separation from the plasma sheet and magnetosheath. The grey tubes are field lines.

At this time, a large part of the tail and almost all of the plasma sheet tailward of about -25 R_E are on IMF field lines. These field lines have undergone reconnection at the near-Earth X-line near -25 R_E, which extends all across the tail between the dawn and dusk magnetopause. The flow velocity in the plasma sheet becomes very high, with tailward flows in some places near the tail center exceeding 1000 km s^{-1}. The lobes, i.e., regions of open field lines, extend to fairly high latitudes and the tail cross section is distinctly elliptical at -200 R_E downtail. Close inspection of the lobe field lines shows that they are all IMF field lines that have reconnected at the dayside magnetopause and have been subsequently swept into the tail by the magnetosheath flow. Closer to the Earth, plasma flows on the closed field lines are mostly sunward (not shown here) and follow a well defined two cell convection pattern.

This flow and the associated magnetic topology closely resemble those of the Dungey [1961] model of an open magnetosphere, in which the magnetospheric convection is entirely driven by reconnection. The main difference in our model is that the tail X-line is closer to the Earth than most observations suggest. Because of the constant driving by the southward IMF and the almost time stationary structure of the magnetosphere at this time the convection pattern seems to resemble a convection bay [Pytte et al., 1978].

Figure 2 shows the same perspective at t=200 min or 80 min after the IMF has turned northward at the dayside magnetopause. Unlike in the previous figure the color coding here represents different magnetic topologies. Green areas are threaded by solar wind field lines, i.e., field lines that are not connected with the Earth. Areas in light blue are threaded by open field lines, i.e., those with one foot on the Earth, and dark blue areas are threaded with closed field lines. Another class of field lines forms closed loops and areas threaded by those field lines are color coded in red. Some selected field lines are drawn to elucidate the magnetic topology. The slight asymmetry of the tail is due to the day – night gradients of the ionospheric Hall conductance that forces a non symmetric ionospheric convection pattern, which in turn breaks the symmetry of the magnetospheric flow.

By this time reconnection has stopped at the dayside magnetopause and started at the high latitude magnetopause close to the terminator between the IMF and lobe field lines. By this reconnection process, which is roughly symmetric in the northern and southern hemispheres new closed field lines are produced on the dayside; these are embedded in magnetosheath plasma. Subsequently, these field lines are swept along the magnetopause into the tail flanks, where they form an extension of the Low Latitude Boundary Layer (LLBL) into the distant tail. This result is similar to that recently reported by Ogino et al. [1994]. The tail X-line continues to exist. However, reconnection has become much weaker and tailward velocities have decreased in most parts of the tail to about 200 km s^{-1}or less. Only in a narrow band, about 10 R_E wide along the center of the tail, does the tailward velocity remain high (400 - 700 km s^{-1}). By this time the X-line has a limited extent in the dawn-dusk direction and does not reach the flank magnetopause any more, as was the case during southward IMF. Another important change is that now tail reconnection occurs with field lines of two different topologies. Near the tail center, lobe field lines reconnect just as they did during the previous southward IMF interval. Further towards the flanks, reconnection occurs on closed field lines which leads to plasmoid-like closed loop structures downstream. This is a new feature that has not been reported from earlier global simulation studies which used shorter tails. Close inspection of these loops shows that they are oriented such that their earthward ends lie closer to the tail axis than their tailward ends. This indicates that the closed boundary layer field lines in the flanks, while their ends are convecting rapidly tailward, also convect towards the tail center at about -25 R_E where they reach the X-line and reconnect. This reconnection occurs at the near-Earth interface of closed field lines and closed loops (the dark blue - red interface in Figure 2) at about -25 R_E. Besides the closed loops near the tail flanks, Figure 2 also shows a plasmoid structure near -80 R_E in the tail center. Inspection of the temporal evolution in the near-Earth plasma sheet (not shown here) shows that these plasmoids develop because the X-line periodically moves tailward to about -50 R_E and reforms near -20 R_E. This occurs on a time scale of about 20 - 30 min. Each time the near-Earth X-line reforms, a plasmoid is formed and ejected tailward. The plasmoids do not uniformly move tailward. Because the flow velocity is larger in the tail center, they are being deformed by the velocity shear and pushed towards the flanks where they join the already existing closed field loops. A more detailed

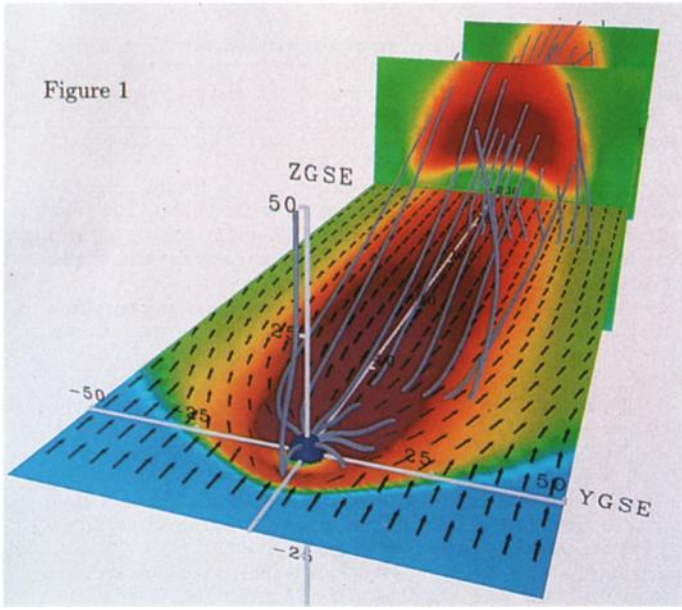

Figure 1. Perspective view of the magnetosphere from a sunward – duskward position at t=120 min. In the equatorial plane the logarithm of the temperature is color coded (lowest temperatures are blue, highest temperatures are red) together with flow vectors. The lenghth of the flow vectors is proportional to the square root of the velocity. The vertical cuts at -200 R_E and -360 R_E are color coded with B_z (red corresponds to 8 nT and green to zero). The grey tubes are field lines.

study of the temporal and spatial behavior of the plasmoids will be presented elsewhere.

Figure 3 displays the tail structure 3 hours and 45 min after the northward turning of the IMF. The format is unchanged from the previous figure and displays the magnetic topology. Although the field topology has not changed, the proportions are now different. The closed field line region in the flanks and

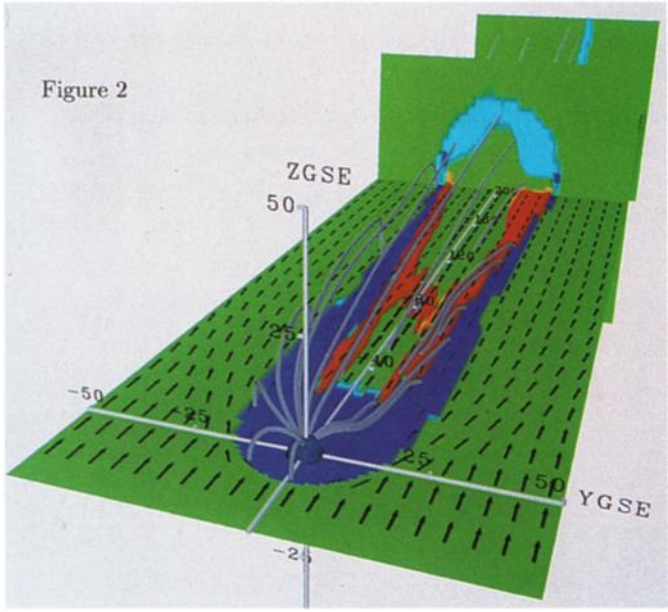

Figure 2. The same perspective as Figure 1 for t = 200 min, 80 min after the northward turning of the IMF. The color coding represents the magnetic topology. Dark blue areas are threaded by closed field lines, light blue areas by open field lines, green areas by solar wind field lines, and red areas by closed loops.

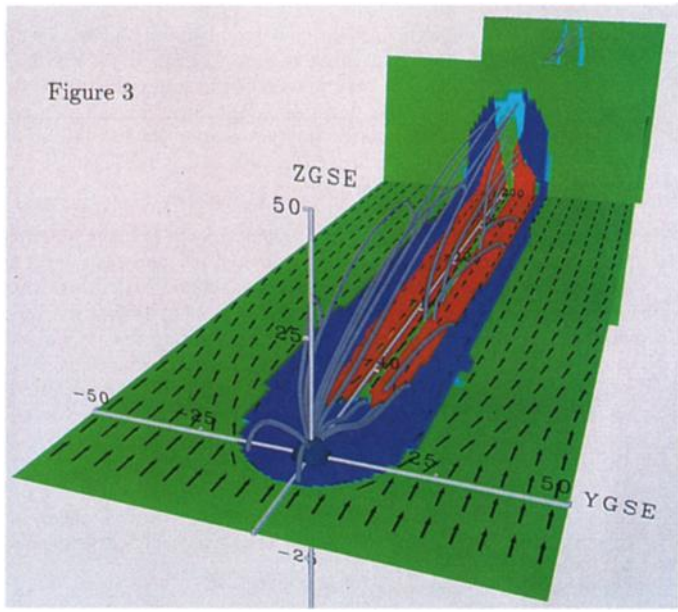

Figure 3. The same as Figure 2 for t = 345 min, 225 min after the northward turning of the IMF.

the closed loop field regions have grown considerably at the expense of the lobe and solar wind field. Reconnection on lobe field lines now occurs only on a very small part of the X-line, which has itself become shorter. By this time the X-line position has become steady and no more plasmoids are being generated. The IMF field lines in the tail center (green) now form a very narrow channel which is only a few R_E wide. The velocity in this channel is considerably higher than in the neighboring closed loop regions. This may be explained by the fact that the plasma properties of the lobe field lines are different from the closed field lines. In particular, the higher Alfvén velocity of the lobes allows for higher reconnection rates and higher outflow speed. The tail lobes now occupy only a small fraction of the tail cross section at high latitudes, while the closed field line region extends to high latitudes and almost engulfs the entire tail. The principal cross sectional structure does not change very much as a function of distance down the tail. It evolves very slowly in time, with the closed field line regions, i.e., the boundary layer of closed field lines and the closed field loops occupying an increasing fraction of the tail volume.

Summary and Discussion

We have used a new global MHD simulation model to study the evolution and structure of the distant geomagnetic tail under long and steady northward IMF conditions. We find that the tail develops a well defined structure after about one solar wind transit time with northward IMF, which persists to at least 400 R_E downstream. The structure and dynamics are distinctly different from periods with southward IMF, but, as for southward IMF, are dominated by magnetic reconnection. There are three regions of magnetic reconnection: the northern and southern high latitude magnetopause, where lobe field lines reconnect with solar wind field lines, and an X-line between -20 and -40 R_E in the center of the tail. Tail reconnection is significantly weaker when the IMF is northward than when it is southward and occurs both on open lobe and closed field lines. As a consequence, the open magnetic flux in the lobes decreases slowly and steadily. However, even after almost 4 hours of northward IMF the lobes persist. Whether or not the lobes will eventually disappear depends on the reconnection rates and the duration of the northward IMF. As a consequence of the reconnection sites at the high latitude magnetopause, new closed field lines are generated and are embedded in the magnetosheath. These field lines convect with the mag-

netosheath flow tailward and are stretched along the flanks of the tail. Although this stretching causes a sunward $j \times B$ force, the momentum flux of the magnetosheath is so large that these lines become stretched to at least 400 R_E down the tail. These field lines form a broad boundary layer in the distant tail that also extends to fairly high latitudes. We call it the Tail Flank Boundary Layer (TFBL) here.

At least some of the field lines of the TFBL undergo magnetic reconnection a second time when they reach the tail X-line. Their tailward parts are then pinched off, and they form a region of closed loop structures just inside the TFBL. Next the closed loops convect slowly (100 - 200 km s^{-1}) tailward. The magnetic topology of the closed loops is similar to that of a plasmoid, with one major difference. While a plasmoid would have an O-line in the dawn-dusk direction, the closed loops are tilted such that their field points southward near the center of the tail and northward near the flanks. This implies the presence of two O-lines aligned with the tail axis and starting at the ends of the tail X-line. The three separator lines enclose a central region of the equatorial plane where the field is southward. Outside of the separator the field is northward (the upward pointing part of the closed loops and the TFBL).

Comparison of our results with observations is difficult because almost all tail observations are statistical, and the existence of a purely northward IMF for an extended time interval is very rare. We may note, however, that our results are consistent with Slavin et al.'s [1985] observations that tailward plasmasheet flows are often seen associated with positive B_z. Also in agreement with these observations, we find negative B_z near the tail axis and positive B_z in the flanks. Unlike Slavin et al. [1985, 1987] however, we interpret the B_z=0 interface between the tail center and the flanks as a topological O-line and only the central part nearest to the Earth as an X-line. Our results are also consistent with recent ISEE 3 observations of the distant tail during periods of northward IMF [Fairfield, 1993] which indicate that the tail narrows in the dawn - dusk direction and forms a boundary layer of plasma with properties intermediate between magnetosheath and tail plasma.

Acknowledgements. This research is supported by NASA grant NAGW-1100 at UCLA. Computations were carried out on the iPSC/860 at the San Diego Supercomputer Center.

References

Dungey, J. W., Interplanetary magnetic field and the auroral zones, *Phys. Rev. Lett., 6*, 47, 1961.

Evans, C. R., and J. F. Hawley, Simulation of magnetohydrodynamic flows: A constrained transport method, *Ap. J., 332*, 659, 1988.

Fairfield, D. H., Solar wind control of the distant magnetotail: ISEE 3, *J. Geophys. Res., 98*, 21265, 1993.

Harten, A., and G. Zwas, Self-adjusting hybrid schemes for shock computations, *J. Comp. Phys., 9*, 568, 1972.

Heikkila, W. J., Neutral-sheet crossings in the distant magnetotail, in *Magnetotail Physics*, edited by A. T. Y. Lui, The John Hopkins University Press, Baltimore, 65, 1987.

Hirsch, C., *Numerical Computation of Internal and External Flows*, Volume II, Wiley, New York, 1990.

Kamide, T., and S. Matsushita, Simulation studies of ionospheric electric fields and currents in relation to field aligned currents, 1, Quiet periods, *J. Geophys. Res., 84*, 4083, 1979.

Ogino, T., R. J. Walker, and M. Ashour-Abdalla, A global magnetohydrodynamic simulation of the response of the magnetosphere to a northward turning of the interplanetary magnetic field, *J. Geophys. Res., in press*, 1994.

Pytte, T., R. L. McPherron, E. W. Hones, and H. I. West, Jr., Multiple satellite studies of magnetospheric substorms: Distinction between polar magnetic substorms and convection driven negative bays, *J. Geophys. Res., 83*, 663, 1978.

Rasmussen, C. E., and R. W. Schunk, Ionospheric convection driven by NBZ currents, *J. Geophys. Res., 92*, 4491, 1987.

Siscoe, G. L., D. G. Sibeck, J. A. Slavin, E. J. Smith, B. T. Tsurutani, and D. E. Jones, ISEE 3 magnetic field observations in the magnetotail: Implications for reconnection, in *Magnetic Reconnection*, Geophys. Monogr. Ser., vol. 30, edited by E. W. Hones, *pp. 240*, AGU, Washington, D.C., 1987.

Slavin, J. A., E. J. Smith, D. G. Sibeck, D. N. Baker, R. D. Zwickl, and S.-I. Akasofu, A ISEE 3 study of average and substorm conditions in the distant magnetotail, *J. Geophys. Res., 90*, 10875, 1985.

Slavin, J. A., P. W. Daly, E. J. Smith, T. R. Sanderson, K. P. Wenzel, R. P. Lepping, and H. W. Kroehl, Magnetic configuration of the distant plasma sheet: ISEE 3 observations, in *Magnetotail Physics*, edited by A. T. Y. Lui, The John Hopkins University Press, Baltimore, 59, 1987.

Tsurutani, B. T., B. E. Goldstein, M. E. Burton, and D. E. Jones, A review of the ISEE 3 geotail magnetic field results, *Planet. Space Sci., 34*, 931, 1986.

Walker, R. C., U. Villante, and A. J. Lazarus, Pioneer 7 observations of plasma flow and field reversal regions in the distant geomagnetic tail, *J. Geophys. Res., 80*, 1238, 1975.

J. Raeder, R. J. Walker, and M. Ashour-Abdalla, IGPP/UCLA, 405 Hilgard Ave, Los Angeles, CA 90024-1567

(Received: April 28, 1994; revised: October 3, 1994; accepted: November 16, 1994)